Inorg. Chem. **2003**, *42*, 5825–5836

Hydrolysis of 4-Nitrophenyl Acetate by a (N_2S(thiolate))zinc Hydroxide Complex: A Model of the Catalytically Active Intermediate for the Zinc Form of Peptide Deformylase

Robert C. diTargiani,[†] SeChin Chang,[†] Michael H. Salter, Jr.,[‡] Robert D. Hancock,[‡] and David P. Goldberg*,[†]

Departments of Chemistry, The Johns Hopkins University, 3400 North Charles Street, Baltimore, Maryland 21218, and University of North Carolina—Wilmington, Wilmington, North Carolina 28403

Received March 29, 2003

A novel zinc(II) hydroxide complex with a rare alkylthiolate donor in the coordination sphere is formed in aqueous solution from the dissolution of the zinc alkyl precursor complex (PATH)$ZnCH_3$ (PATH = 2-methyl-1-[methyl(2-pyridin-2-ylethyl)amino]propane-2-thiolate) in H_2O and protonolysis of the Zn–C bond to give (PATH)ZnOH (**1**). The (PATH)ZnOH complex has been shown to promote the hydrolysis of 4-nitrophenyl acetate (4-NA) by a detailed kinetic study and is the first functional model for the zinc form of the enzyme peptide deformylase. From a fit of the sigmoidal pH–rate profile a kinetic pK_a of 8.05(5) and a pH-independent second-order rate constant (k''_{max}) of 0.089(3) M^{-1} s^{-1} have been obtained. The kinetic pK_a is similar to the pK_a of 7.7(1) determined by a potentiometric study (25 °C, I = 0.1 ($NaNO_3$)). Observation of both rate enhancement and turnover shows that **1** acts as a catalyst for the hydrolysis of 4-NA, although the turnovers are modest. Activation parameters have been obtained from a temperature-dependence study of the rate constants (E_a = 54.8 kJ mol^{-1}, $\Delta H^{\ddagger}$ = 52.4 kJ mol^{-1}, and $\Delta S^{\ddagger}$ = –90.0 J mol^{-1} K^{-1}), and support a reaction mechanism which depends on nucleophilic attack of **1** in the rate-determining step. This is the first kinetic and thermodynamic study of a 4-coordinate zinc hydroxide complex containing a thiolate donor. In addition it is only the second time that a complete set of activation parameters have been obtained for the zinc-promoted hydrolysis of a carboxylic ester. This study puts the basicity and nucleophilicity of a (N_2S)ZnOH complex in context with those of other L_nZnOH complexes and enzymes.

Introduction

The synthesis and study of small-molecule models of mononuclear zinc enzymes such as carbonic anhydrase, thermolysin, and alcohol dehydrogenase has greatly improved our understanding of the mechanisms of action of these systems.[1] For example, the prototypical zinc enzyme carbonic anhydrase (CA) contains a zinc(II) ion in the active site bound by three histidine residues and a catalytically active water molecule ($(His)_3Zn(OH_2)$).[2] Model complexes of carbonic anhydrase prepared from various polydentate nitrogen donor ligands have been instrumental in understanding the active site structure and mechanism of this enzyme.[3] It was believed for a number of years that the enzyme peptide deformylase (PDF), which is found mostly in prokaryotes, belonged to the same family of zinc enzymes as carbonic anydrase.[4] PDF contains the conserved HEXXH sequence found in mononuclear zinc proteins, and the metal ion

* Author to whom correspondence should be addressed. E-mail: dpg@jhu.edu.
[†] The Johns Hopkins University.
[‡] University of North Carolina—Wilmington.

(1) (a) Chin, J. *Acc. Chem. Res.* **1991**, *24*, 145−152. (b) Suh, J. *Acc. Chem. Res.* **1992**, *25*, 273−279. (c) Kimura, E. In *Progress in Inorganic Chemistry*; Karlin, K. D., Ed.; John Wiley & Sons: New York, 1994; Vol. 41, pp 443−491. (d) Vahrenkamp, H. *Acc. Chem. Res.* **1999**, *32*, 589−596. (e) Parkin, G. *Chem. Commun.* **2000**, 1971−1985. (f) Kimura, E. *Acc. Chem. Res.* **2001**, *34*, 171−179.

(2) (a) Christianson, D. W.; Cox, J. D. *Annu. Rev. Biochem.* **1999**, *68*, 33−57. (b) Tripp, B. C.; Smith, K.; Ferry, J. G. *J. Biol. Chem.* **2001**, *276*, 48615−48618.

(3) See for example: (a) Kimura, E.; Shiota, T.; Koike, T.; Shiro, M.; Kodama, M. *J. Am. Chem. Soc.* **1990**, *112*, 5805−5811. (b) Xu, X.; Lajmi, A. R.; Canary, J. W. *Chem. Commun.* **1998**, 2701−2702. (c) Bergquist, C.; Parkin, G. *J. Am. Chem. Soc.* **1999**, *121*, 6322−6323. (d) Kimblin, C.; Murphy, V. J.; Hascall, T.; Bridgewater, B. M.; Bonanno, J. B.; Parkin, G. *Inorg. Chem.* **2000**, *39*, 967−974. (e) Sprigings, T. G.; Hall, C. D. *J. Chem. Soc., Perkins Trans. 2* **2001**, 2063−2067. (f) Sénèque, O.; Rager, M.-N.; Giorgi, M.; Reinaud, O. *J. Am. Chem. Soc.* **2001**, *123*, 8442−8443.

10.1021/ic034337o CCC: $25.00
Published on Web 08/16/2003

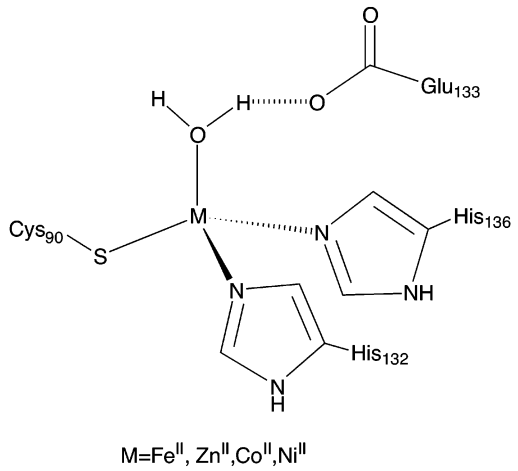

Figure 1. Structure of the active site of peptide deformylase.

coordination sphere matches that of the zinc enzyme family (three amino acid ligands + one H_2O molecule).[5] Moreover, PDF catalyzes the hydrolysis of a formyl group from the N-terminus of newly formed polypeptides, which corresponds in general to the hydrolytic function of many of the other zinc enzymes, including other peptidases such as thermolysin[6] and carboxypeptidase A.[7] Thus, it is quite surprising that there is now a large body of evidence to suggest that PDF in fact contains iron(II), and not zinc(II), as the metal ion in vivo.[8] The inner coordination sphere of the catalytically active metal is comprised of a N_2S(thiolate) ligand set, [His_2-$CysM^{II}(OH_2)$], as shown in Figure 1. The structures of Zn^{II}-, Co^{II}-, Ni^{II}-, and Fe^{II}PDF are all essentially identical as determined by high-resolution X-ray crystallography.[8c,d,9] However, Zn^{II}PDF is dramatically less active than Co^{II}-, Ni^{II}-, and Fe^{II}PDF in the hydrolysis of formamide substrates.[8,10]

We have recently synthesized a new family of structural analogues of the PDF active site. These model complexes contain the requisite N_2S(thiolate) coordination sphere provided by the pyridine−amine−thiolate ligand 2-methyl-1-[methyl(2-pyridin-2-ylethyl)amino]propane-2-thiolate (PATH) and are of the type (PATH)$M^{II}X$, where M = Zn and Co and X = Br and NCS and M = Zn and X = O_2CR and CH_3.[11−13] Prior to the synthesis of these complexes, there were very few examples of monomeric, tetrahedral zinc(II) or cobalt(II) complexes with a mixed N/S(thiolate) donor set and a fourth labile site.[14] The synthetic challenge in making accurate structural models of PDF comes from the difficulties of preparing monomeric complexes with a mixed N,S donor set.[15] Although there are several known examples of polydentate, homoleptic nitrogen donor ligands that give monomeric complexes with zinc(II) and other divalent metals (see Chart 1), there are very few ligands which provide a heteroleptic N/S(thiolate) donor set and have been shown to give monomeric M^{II} complexes.[14] In particular, alkylthiolates are very difficult to incorporate in monomeric complexes because of their great tendency to form M−S(R)−M bridged structures, and because they are easily oxidized to disulfides and other products. In addition, most of the enzymes in the zinc enzyme family contain all-nitrogen, or mixed nitrogen/oxygen donor sets from the amino acids histidine and glutamate or aspartate (e.g., CA, thermolysin, carboxypeptidase A),[5] and thus, there has not been as much effort to incorporate thiolate donors in zinc model systems, with the exception of some recent models of alcohol dehydrogenase and the cysteine-containing DNA repair enzyme Ada from *E. coli*.[16]

In this work we describe the generation of a N_2S(thiolate)-zinc hydroxide complex in aqueous solution with the PATH ligand, and present an in-depth study of the hydrolysis of 4-nitrophenyl acetate (4-NA). To our knowledge, this is the first example of a 4-coordinate zinc species that contains an alkylthiolate donor in the coordination sphere and is capable of promoting hydrolysis. Although 4-NA is considerably easier to hydrolyze than the native formamide substrate of PDF, the hydrolysis of this substrate by (PATH)ZnOH serves as a generalized model for the hydrolytic reactivity of a zinc hydroxide unit in a N_2S(thiolate) environment, which has

(4) (a) Meinnel, T.; Blanquet, S. *J. Bacteriol.* **1995**, *177*, 1883−1887. (b) Meinnel, T.; Lazennec, C.; Blanquet, S. *J. Mol. Biol.* **1995**, *254*, 175−183. (c) Meinnel, T.; Blanquet, S.; Dardel, F. *J. Mol. Biol.* **1996**, *262*, 375−386.
(5) (a) Hooper, N. M. *FEBS Lett.* **1994**, *354*, 1−6. (b) Lipscomb, W. N.; Sträter, N. *Chem. Rev.* **1996**, *96*, 2375−2433.
(6) Matthews, B. W. *Acc. Chem. Res.* **1988**, *21*, 333−340.
(7) Christianson, D. W.; Lipscomb, W. N. *Acc. Chem. Res.* **1989**, *22*, 62−69.
(8) (a) Rajagopalan, P. T. R.; Yu, X. C.; Pei, D. *J. Am. Chem. Soc.* **1997**, *119*, 12418−12419. (b) Groche, D.; Becker, A.; Schlichting, I.; Kabsch, W.; Schultz, S.; Wagner, A. F. V. *Biochem. Biophys. Res. Commun.* **1998**, *246*, 342−346. (c) Becker, A.; Schlichting, I.; Kabsch, W.; Groche, D.; Schultz, S.; Wagner, A. F. V. *Nat. Struct. Biol.* **1998**, *5*, 1053−1058. (d) Baldwin, E. T.; Harris, M. S.; Yem, A. W.; Wolfe, C. L.; Vosters, A. F.; Curry, K. A.; Murray, R. W.; Bock, J. H.; Marshall, V. P.; Cialdella, J. I.; Merchant, M. H.; Choi, G.; Deibel, M. R. *J. Biol. Chem.* **2002**, *277*, 31163−31171.
(9) (a) Chan, M. K.; Gong, W.; Rajagopalan, P. T. R.; Hao, B.; Tsai, C. M.; Pei, D. *Biochemistry* **1997**, *36*, 13904−13909. (b) Becker, A.; Schlichting, I.; Kabsch, W.; Schultz, S.; Wagner, A. F. V. *J. Biol. Chem.* **1998**, *273*, 11413−11416. (c) Hao, B.; Gong, W.; Rajagopalan, P. T. R.; Zhou, Y.; Pei, D.; Chan, M. K. *Biochemistry* **1999**, *38*, 4712−4719.
(10) Rajagopalan, P. T. R.; Grimme, S.; Pei, D. *Biochemistry* **2000**, *39*, 779−790.
(11) Chang, S. C.; Karambelkar, V. V.; Sommer, R. D.; Rheingold, A. L.; Goldberg, D. P. *Inorg. Chem.* **2002**, *41*, 239−248.
(12) Chang, S.; Sommer, R. D.; Rheingold, A. L.; Goldberg, D. P. *Chem. Commun.* **2001**, 2396−2397.
(13) Chang, S.; Karambelkar, V. V.; diTargiani, R. C.; Goldberg, D. P. *Inorg. Chem.* **2001**, *40*, 194−195.
(14) (a) Hammes, B. S.; Carrano, C. J. *J. Chem. Soc., Dalton Trans.* **2000**, 3304−3309. (b) Hammes, B. S.; Carrano, C. J. *Inorg. Chim. Acta* **2000**, *300*−*302*, 427−433. (c) Hammes, B. S.; Carrano, C. J. *Inorg. Chem.* **2001**, *40*, 919−927.
(15) (a) Ghosh, P.; Parkin, G. *Chem. Commun.* **1998**, 413−414. (b) Shoner, S. C.; Nienstedt, A. M.; Ellison, J. J.; Kung, I. Y.; Barnhart, D.; Kovacs, J. A. *Inorg. Chem.* **1998**, *37*, 5721−5726. (c) Chiou, S. J.; Innocent, J.; Riordan, C. G.; Lam, K. C.; Liable-Sands, L.; Rheingold, A. L. *Inorg. Chem.* **2000**, *39*, 4347−4353.
(16) For recent examples, see: (a) Bergquist, C.; Storrie, H.; Koutcher, L.; Bridgewater, B. M.; Friesner, R. A.; Parkin, G. *J. Am. Chem. Soc.* **2000**, *122*, 12651−12658. (b) Seebacher, J.; Shu, M. H.; Vahrenkamp, H. *Chem. Commun.* **2001**, 1026−1027. (c) Bergquist, C.; Koutcher, L.; Vaught, A. L.; Parkin, G. *Inorg. Chem.* **2002**, *41*, 625−627. (d) Garner, D. K.; Fitch, S. B.; McAlexander, L. H.; Bezold, L. M.; Arif, A. M.; Berreau, L. M. *J. Am. Chem. Soc.* **2002**, *124*, 9970−9971. (e) Garner, D. K.; Allred, R. A.; Tubbs, K. J.; Arif, A. M.; Berreau, L. M. *Inorg. Chem.* **2002**, *41*, 3533−3541. (f) Makowska-Grzyska, M. M.; Jeppson, P. C.; Allred, R. A.; Arif, A. M.; Berreau, L. M. *Inorg. Chem.* **2002**, *41*, 4872−4887. (g) Wilker, J. J.; Lippard, S. J. *Inorg. Chem.* **1997**, *36*, 969−978. (h) Warthen, C. R.; Hammes, B. S.; Carrano, C. J.; Crans, D. C. *J. Biol. Inorg. Chem.* **2001**, *6*, 82−90.

Chart 1

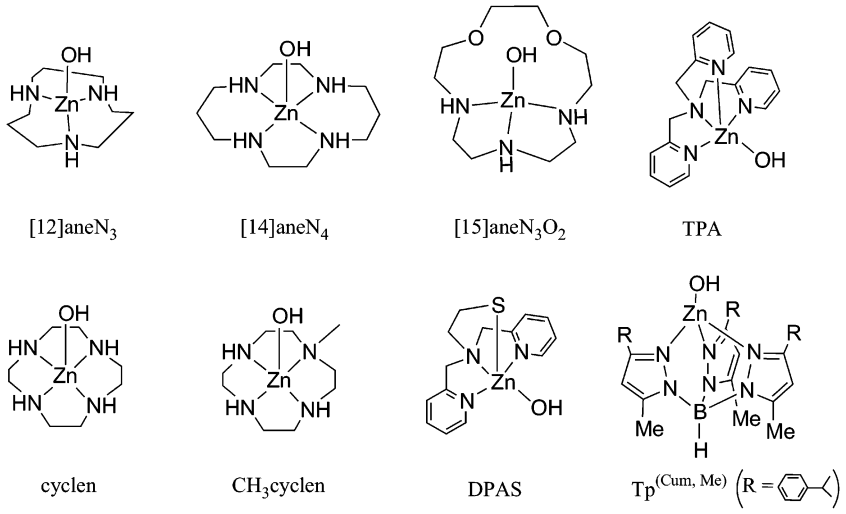

direct relevance to the catalytically active $M^{II}OH$ unit in proposed mechanisms of PDF.[8,10]

A metal-bound hydroxide is now accepted as the reactive intermediate in the mechanism of many zinc enzymes, and thus, there has been a particular focus by several research groups on the preparation of L_nZnOH complexes and their reactivity toward various substrates such as CO_2, organophosphate esters, and carboxylic esters including 4-NA. One likely role for the metal ion in zinc enzymes and in PDF is to lower the pK_a of the catalytically active water molecule to yield a powerful nucleophile, L_nZnOH, as a reactive intermediate. Thus, the pK_a of L_nZnOH model complexes is an important parameter to quantify, and it is of interest to delineate what structural factors at the metal center (e.g., donor type) help to determine this pK_a value. In this work we have obtained for the first time the pK_a of a (N_2S-(thiolate)ZnOH complex from both kinetic (pH−rate profile) and thermodynamic (potentiometric titration) measurements, allowing us to make comparisons with a series of zinc models and proteins. A mechanism for ester hydrolysis is proposed that relies on (PATH)ZnOH acting as a simple nucleophile toward 4-NA, and the hydrolytic efficiency (k''_{max}) and hence nucleophilicity of this species have been obtained and compared with those of other zinc model complexes. In addition, activation parameters for the hydrolysis reaction, including $\Delta H^{\ddagger}$ and $\Delta S^{\ddagger}$, have been obtained from a temperature dependence of the rate constants. This is only the second time that detailed activation parameters have been obtained for the hydrolysis of an ester by a zinc complex, and the values of these parameters are consistent with the proposed mechanism. Part of our long-term interest lies in determining what properties of the metal center might explain the remarkably low reactivity of the zinc form of PDF. Given that the Fe^{II} and Zn^{II} forms of PDF are essentially isostructural, it is reasonable to postulate that there are inherent properties of the MOH unit (e.g., pK_a, nucleophilicity) that are responsible for the large drop in reactivity on going from iron to zinc. We have quantified some of these properties for the model complex in this study.

Experimental Section

General Considerations. PATH−H[11] and (PATH)$ZnCH_3$ (**2**)[12] were prepared as previously described. Good's buffers HEPES (*N*-1-hydroxyethylpiperazin-*N*′-2-ethanesulfonic acid) and CHES (2-(cyclohexylamino)propanesulfonic acid) were obtained from Sigma and used without further purification. HEPES-d_{18} (98 atom %) was obtained from Cambridge Isotope Laboratories, Inc. 4-Nitrophenyl acetate (Aldrich) and sodium 4-nitrophenolate (Acros) were obtained and used without further purification. All other reagents were obtained from commercial sources and used as received. ^{1}H NMR spectra were recorded on a Varian Unity plus 400 spectrometer (400 MHz) or a Bruker AMX-300 spectrometer (300 MHz). Tetramethylsilane in organic solvents and HOD (4.80 ppm) in D_2O were used as internal references for ^{1}H NMR measurements. Kinetic studies were carried out by a visible spectral method using an Agilent 8453 photodiode-array spectrophotometer equipped with a thermostatable cell holder and the Agilent biochemical analysis software package.

(PATH)ZnOH (1). A sample of **2** (0.050 g, 0.167 mmol) was slowly dissolved in 4 mL of D_2O and stirred for 14 h. At the end of this period there was a very small amount of white powder remaining, which was presumably a small quantity of unreacted starting material. The solution was filtered through a Celite plug and diluted with D_2O to a total volume of 5.00 mL. The final concentration of this stock solution was calculated by ^{1}H NMR spectroscopy in the following manner. To 300 μL of the stock solution of **1** was added 300 μL of a stock solution of NaOAc (30 mM) in D_2O. The ^{1}H NMR spectrum of this solution was recorded, and the integrated area of the methyl peak (δ 1.90 ppm) of sodium acetate was compared with the integrated area of several peaks from **1** to obtain the final concentration of **1**. Typical values ranged between 28 and 32 mM. This solution was then used as the source of **1** for all hydrolysis experiments. The concentration of this stock solution was periodically checked by ^{1}H NMR, and no change in concentration was observed over a 2-week period. ^{1}H NMR (D_2O): δ (ppm) 1.24 (s, 3H, CH_3), 1.45 (s, 3H, CH_3), 2.57 (d, 1H, $-CH_2-$), 2.70 (s, 3H, NCH_3), 2.81 (d, 1H, $-CH_2-$), 2.99 (m, 1H, $-CH_2-$), 3.14 (m, 3H, $-CH_2-$), 7.53 (m, 2H, H_β and H_δ), 8.01 (t, 1H, H_γ), 8.50 (d, 1H, H_α).

Potentiometric Titrations. Potentiometric titrations were carried out in an air-tight glass cell flushed with N_2 gas, and thermostated to 25.0 ± 0.1 °C. All titrations were carried out in a background of 0.1 M $NaNO_3$. The pH values for the titrations were monitored

Table 1. Protonation and Formation Constants Calculated for PATH−H (L) and PATH−H and Zinc(II) in 0.1 M $NaNO_3$ at 25.0 °C, along with Formation Constants for Other Ligands

equilibrium	log *K*	ref
$H^+ + OH^- \rightleftarrows H_2O$	13.78	a
$L^- + H^+ \rightleftarrows HL$	10.50(5)	this work
$HL + H^+ \rightleftarrows H_2L^+$	7.00(2)	this work
$H_2L^+ + H^+ \rightleftarrows H_3L^{2+}$	3.21(2)	this work
$Zn^{2+} + L^- \rightleftarrows ZnL^+$	10.35(2)[b]	this work
$ZnL^+ + OH^- \rightleftarrows ZnLOH$	6.1(1)	this work
$ZnL(OH_2)^+ \rightleftarrows ZnLOH + H^+$	−7.7(1)	this work
log *K*(ZnL) for Other Zn Complexes		
[12]aneN_3	8.4	3a
cyclen	15.3(1)	30
[15]aneN_3O_2	9.0(1)	28
[14]aneN_4	15.5	3a

[a] Martell. A. E.; Smith, R. M. *Critical Stability Constants*; Plenum: New York, 1974, 1989; Vols. 1 and 5. [b] log *K*(ZnL).

using an Orion model 8172 BN glass electrode coupled with a VWR SR601C pH meter capable of reading to 0.1 mV. The glass electrode was standardized by determining $E°$ (the standard potential for the cell) by acid−base titration, which allowed for a determination of the Nernstian slope applicable to the system. The PATH−H ligand was found to be unstable in solutions kept for more than a few days. As a precaution, fresh PATH−H solutions were made up for each titration, and standardized by titration with a standard acid solution. Titrations typically showed the PATH−H to be in excess of 99% pure. ^{13}C NMR spectra of the PATH−H titration solutions were run before and after each titration to ensure that no detectable deterioration of the ligand had occurred during the titration. The pure PATH−H ligand itself was kept refrigerated at −81 °C, which was found to prevent decomposition. The protonation constants of PATH−H were determined by routine glass-electrode titration methods.[17] Titrations were carried out with total Zn concentrations ranging from 0.0067 to 0.0036 M, and PATH:Zn ratios between 1.46:1 and 1.42:1. In all, four separate titrations were carried out. For each titration, the values of $\bar{n}$ (the ratio of the concentration of ligand bound to the concentration of metal ion) were calculated.[18] It was found that the four $\bar{n}$ versus log [L] curves showed good superimposability, and fitted a simple model where only a ZnL complex was present. At $\bar{n}$ values above 1.0, the $\bar{n}$ curve rose again to a higher value, which corresponded to the formation of (PATH)-ZnOH. The calculated protonation constants for PATH−H and formation constants of PATH−H with Zn(II) are given in Table 1.

Hydrolysis of 4-NA. Product Analysis. In an NMR tube, an amount of **1** (420 μL of a 14.3 mM stock solution in D_2O) was combined with 120 μL of a stock solution of HEPES-d_{18} and $NaClO_4$ (100 and 500 mM in D_2O, respectively), and then 4-NA (60 μL of a 100 mM stock solution in CD_3CN) was added, giving a final pH of 8.2. The NMR spectrum was recorded 5 min, 3 h, and 9 h after the addition of 4-NA. After 9 h, only the peaks for the (PATH)Zn complex, 4-nitrophenolate (4-NP), and acetate were observed.

Hydrolysis of 4-NA. Kinetics. The rate of hydrolysis of 4-NA promoted by **1** in H_2O/CH_3CN (90:10 v/v) in the pH range 7.0−9.5 was measured by an initial rate method. The reaction was monitored by following the increase in absorbance at 400 nm, corresponding to the appearance of the product 4-NP, up to a 3% yield of 4-NP. The observed extinction coefficients for 4-NP vary with pH as shown by Zhu et al.,[19] and were adjusted accordingly. The pH was maintained by using HEPES (pH 7.0−8.1) or CHES (pH 8.6−9.5) buffer at 20 mM. Ionic strength was maintained by $NaClO_4$ at 100 mM. A typical experiment consisted of loading a UV−vis cell (3.0 mL) with 300 μL of a 4-NA stock solution (10 mM in CH_3CN) and then simultaneously injecting 600 μL of a stock solution containing the appropriate buffer and $NaClO_4$ (100 and 500 mM, respectively) and 2.1 mL of a stock solution of **1** (1.43 mM). The stock solution of **1** used in all the kinetic runs was prepared within two weeks of taking measurements to avoid any decomposition. The concentration of (PATH)Zn complex ([(PATH)-$Zn]_t$) was varied (0.5−4 mM) with constant [4-NA] (1 mM), and [4-NA] was varied (0.5−1 mM) with constant [**1**] (1 mM). A plot of A(400 nm) vs time was linear in all cases, and the slope of the best-fit line gave the observed reaction rate, ν_{init}. The background reaction rate (no metal complex present), ν_{buffer}, was measured at pH 8.1, 8.6, 9.0, and 9.5 (the background rate is only significant above pH 8.1) and subtracted from the observed reaction rate, yielding the desired reaction rate dependent only on the metal complex, $\nu_{[(PATH)Zn]_t}$. The observed second-order rate constants k_{obs} (M^{-1} s^{-1}) were determined as described in the Results. The pH of the reaction mixture was measured before and after the addition of 10% CH_3CN, and no change greater than 0.03 was observed. Thus, no correction was applied for the presence of CH_3CN. At each pH, reaction rates were typically obtained in triplicate (the variation in k_{obs} was found to be ±10%).

Turnover. A reaction mixture of **1** (0.1 mM), 4-NA (5.0 mM), CHES (20 mM, pH 8.6), and $NaClO_4$ (0.1 M) was prepared and allowed to stir at 25 °C for 1 week. During this period aliquots of the reaction mixture (100 μL) were removed daily and diluted to 10 mL. The UV−vis spectrum of the diluted sample was recorded. At the same time an identical reaction was run in the absence of metal complex to measure the amount of background hydrolysis. Turnover numbers were determined by subtraction of the background absorbance from the experimental absorbance, and the difference was multiplied by the dilution factor and divided by the extinction coefficient to yield the amount of 4-NP generated by **1**. The concentration of 4-NP thus obtained was divided by the concentration of (PATH)Zn complex to calculate the turnover number.

Results

Formation of (PATH)ZnOH from (PATH)ZnCH_3. Dissolution of **2** in H_2O results in the quantitative formation of **1** via protonolysis of the Zn−CH_3 bond, as shown in Scheme 1. Previously, we had shown that **1** could be formed in methanol by a substitution reaction involving excess NaOH and (PATH)ZnBr (**3**) in CD_3OD as monitored by ^1H NMR spectroscopy.[11] However, this substitution method was not useful for further reactivity studies since the Br^- still present in solution can compete with OH^-/H_2O for binding to zinc and thus introduces uncertainty as to the identity of the species present at a given pH. In addition, we wanted an aqueous, not methanolic, solution of **1** to promote the hydrolysis of the model substrate 4-NA. In an earlier report we showed that **2** was a useful synthon in the preparation of other monomeric (PATH)ZnX compounds through protonolysis with HX and loss of methane.[12] Thus, the zinc alkyl

(17) Martell, A. E.; Hancock, R. D. *Metal Complexes in Aqueous Solutions*; Plenum Press: New York, 1996.
(18) Girolami, G. S.; Rauchfuss, T. B.; Angelici, R. J. *Synthesis and Technique in Inorganic Chemistry*; University Science Books: Sausolito, CA, 1999.
(19) Zhu, S. R.; Chen, W. D.; Lin, H. K.; Yin, X. C.; Kou, F. P.; Lin, M. R.; Chen, Y. T. *Polyhedron* **1997**, *16*, 3285−3291.

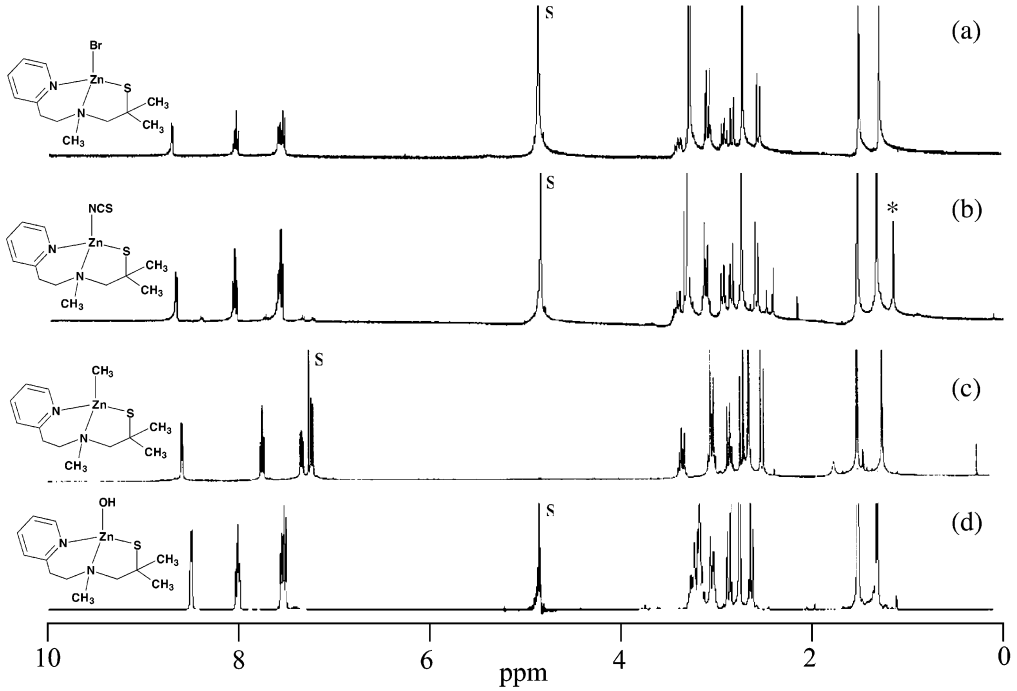

Figure 2. ^{1}H NMR spectra of (PATH)ZnL complexes at room temperature: (a) (PATH)ZnBr in CD_3OD; (b) (PATH)ZnNCS in CD_3OD; (c) (PATH)-$ZnCH_3$ in $CDCl_3$; (d) (PATH)ZnOH in D_2O. Residual solvent is marked by an "s", and minor impurity is marked by an asterisk.

Scheme 1

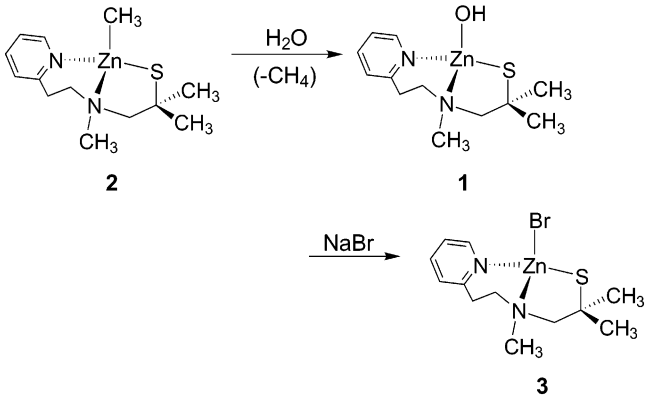

2 appealed to us as a good candidate for the clean formation of **1**. Initially, attempts were made to generate **1** by the addition of H_2O to **2** in organic solvents (e.g., CH_3CN, toluene). These reactions invariably led to the formation of a large amount of a white precipitate, which was only sparingly soluble in H_2O and completely insoluble in other common organic solvents. This material likely contains a small amount of **1** as evidenced by ^{1}H NMR spectroscopy in D_2O (data not shown), in addition to intractable polymeric species (e.g., zinc hydroxides). However, we found that slow dissolution of **2** in pure D_2O gave a clear, homogeneous solution of **1** with only very minor formation of insoluble precipitates.

The ^{1}H NMR spectrum of **1** is shown in Figure 2 together with spectra from other (PATH)ZnX ($X = Br^-$, NCS^-, CH_3) compounds. The monomeric structures for the bromide, thiocyanate, and methyl complexes have all been characterized by X-ray crystallography.[11−13] Each of these compounds exhibits a characteristic diastereotopic pattern in the ^{1}H NMR spectrum distinct from that of free ligand and indicative of a monomeric zinc complex. For example, a singlet at 1.30 ppm is observed for the *gem*-dimethyl groups of the free ligand, but two distinct singlets are seen at ∼1.4 and ∼1.6 ppm for (PATH)ZnX complexes, including **1**, which has two singlets for these groups at 1.43 and 1.61 ppm. The resonances for the pyridine ring protons (H_α, 8.50 ppm; H_γ, 8.01 ppm; $H_{\beta,\delta}$, 7.53 ppm) and ligand backbone resonances (2.57−3.14 ppm) for the hydroxide complex are also quite similar to those of the other monomeric (PATH)Zn complexes. The ^{1}H NMR spectrum of **1**, in comparison to the series of other (PATH)ZnX compounds, provides strong evidence for the proposed monomeric structure. Moreover, a concentration-dependence study of the ^{1}H NMR spectrum of (PATH)ZnOH has been performed, and no change in the spectrum was observed throughout a wide range (1−30 mM). The NMR spectrum of **1** provides a means for quantitating the absolute concentration of **1** by NMR integration against an internal standard (sodium acetate). Thus, a measured amount of NaO_2CCH_3 was added to a freshly prepared solution of **1** in D_2O, and the integrated intensities of several peaks for **1** were compared to that of the singlet at δ 1.90 ppm for the acetate anion. By this method the conversion of the zinc alkyl complex **2** to the hydroxide complex **1** was shown to be quantitative (yield of **1** ∼95% based on **2**).

Conversion of (PATH)ZnOH to (PATH)ZnBr. Complexes of the type (PATH)ZnX are stable to substitution reactions at the X position. We have already shown that a hydroxide complex can be generated by substitution of Br^- in **3** with excess OH^-.[11] The reverse reaction also proceeds in a quantitative fashion. A solution of **1** (0.064 M) freshly prepared in water from **2** was reacted with excess NaBr (0.79

g, 20 equiv) at room temperature. A clear solution was observed for the first 5 min after mixing, at which point a white powder precipitated from the reaction mixture. The reaction was stirred for an additional 30 min, and then the white powder was isolated by filtration, washed with water and Et_2O, and dried under vacuum. A ^1H NMR spectrum of this product in $CDCl_3$, together with its solubility properties (freely soluble in $CDCl_3$, insoluble in water), confirmed that it is the desired complex **3** (final yield 60% based on **2**). This result supports the conclusion that **1** has the monomeric structure shown in Scheme 1.

Potentiometric Titration Studies and Accompanying NMR Measurements. The generation of **1** in situ from the structurally well-defined precursor **2** is a convenient method for obtaining an aqueous solution of pure **1**. Alternatively, a common method of forming an (L)MOH/OH_2 complex involves potentiometric titration via addition of base to an acidic solution of the ligand ($L{\cdot}nH^+$) in the presence of added metal ion, resulting in the formation of $[(L)M]^{n+}$ and $[(L)MOH]^{n+}$ above a certain pH. In addition, such a titration can provide useful thermodynamic information such as ligand/metal formation constants and protonation constants for coordinated water molecules. To obtain this information, we have completed a potentiometric study of the (PATH)-Zn^{II} system in aqueous solution.

The plots in Figure 3 show the potentiometric titration curves for a solution of PATH−H·$2HNO_3$ (a) and PATH−H·$2HNO_3$ in the presence of $Zn(NO_3)_2$ (1.42−1.46 equiv) (b), with 0.1 M $NaNO_3$ in water at 25.0 ± 0.1 °C. The titration data were analyzed according to the equilibria given in Table 1. The second and third protonation constants for PATH−H (log K = 7.00(2) and 3.21(2)) can be assigned to protonation of the secondary amine and pyridine groups, respectively, and are in general agreement with literature values. The first protonation constant (log K = 10.50(5)), which corresponds to the thiol group, is similar to that of ethanethiol (log K = 10.61),[20] but contrasts the lower value determined for the alkylthiol group in the N/S(thiolate) DPAS ligand (log K = 9.2(2))[21] (Chart 1). In Figure 3b the titration data are plotted as a function of $\bar{n}$ (ratio of the concentration of ligand bound to the concentration of total metal ion) versus pH. The data were modeled by using the equilibria given in Table 1, which include the formation of a 1:1 $[(PATH)Zn]^+$ complex (log K(ZnL) = 10.35(5)). The rise in the curve above $\bar{n}$ = 1.0 corresponds to the deprotonation of a coordinated water molecule to give (PATH)ZnOH (pK_a = 7.7(1)). Some complex precipitation occurred at pH > 8.0, preventing further data collection in the alkaline region. It was unnecessary to include equilibria involving other (PATH)Zn^{II} species (e.g., a 2:1 ($PATH_2Zn$) complex or a dimeric ($PATH_2Zn_2$) species) to obtain a good model.

The same mixture used for potentiometric studies was also examined by NMR spectroscopy to obtain structural information on the species in solution. The ^1H NMR spectrum of a 1:1 mixture of PATH−H and $Zn(NO_3)_2$ in the presence of 0.1 M $NaNO_3$ at pH 7.7 in D_2O was collected and showed peaks characteristic of **1**. At this pH there should be a mixture of the zinc aquo and zinc hydroxo species, but it is presumed that they are in rapid equilibrium and give rise to an averaged spectrum. The total concentrations of PATH−H and Zn^{II} were varied between 0.001 and 0.02 mM while the PATH−H:Zn ratio was kept close to 1:1 to check for any dimerization. The spectra do not change with concentration, which is consistent with the presence of a monomeric complex over the entire concentration range.

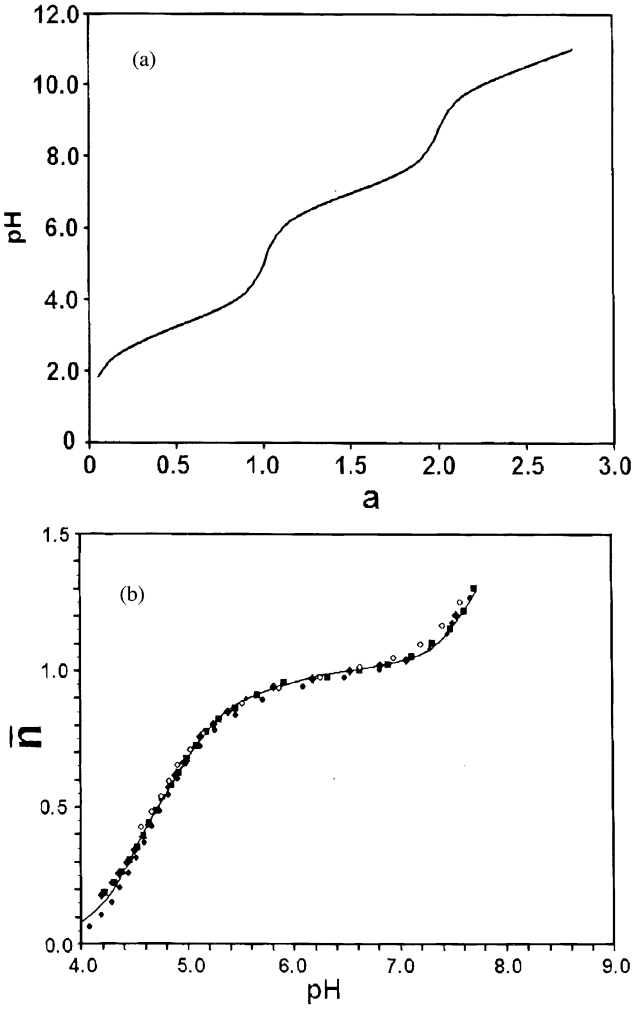

Figure 3. Plots obtained for the titration of (a) PATH−H·$2HNO_3$ (10 mM) against NaOH (1 mM), where a = moles of base added per mole of ligand, and (b) $Zn^{II}(NO_3)_2$ + PATH−H, where $\bar{n}$ = the ratio of the concentration of ligand bound to the metal ion to total metal ion concentration (T = 25 ± 0.5 °C, aqueous, I = 0.1 M $NaNO_3$). The $\bar{n}$ values are calculated from the appropriate mass-balance equations. The solid line is the theoretical $\bar{n}$ versus pH curve as calculated from the protonation constants and formation constants for the system as presented in Table 1.

Hydrolysis of 4-NA. Product Analysis. The substrate 4-NA was chosen to test the hydrolytic efficiency of **1** because it has been used to measure the hydrolytic efficiency of many other zinc model complexes (see Chart 1 and Table 2), and thus serves as a benchmark substrate for calibrating the hydrolytic power of **1**. Before proceeding with the kinetic measurements, the products of this reaction were established by ^1H NMR spectroscopy. Care was taken to keep the

(20) Serjeant, E. P.; Dempsey, B. *Ionisation Constants of Organic Acids in Aqueous Solution;* Pergamon Press: Oxford, 1979.
(21) Kurosaki, H.; Tawada, T.; Kawasoe, S.; Ohashi, Y.; Goto, M. *Bioorg. Med. Chem. Lett.* **2000**, *10*, 1333−1337.

Table 2. Comparison of the pK_a Values and Second-Order Rate Constants k''_{max} (M^{-1} s^{-1}) for Hydrolysis of 4-NA by Various Zinc Model Complexes and Enzymes

	pK_a	k''_{max} (M^{-1} s^{-1})	ref
OH^-	15.7	9.5	43
	Complexes		
(PATH)ZnOH	8.05(5)	0.089 ± 0.003	this work
([12]aneN$_3$)ZnOH	7.3	0.036 ± 0.003[a]	25
(cyclen)ZnOH	7.9	0.1 ± 0.01[a]	26
(CH$_3$cyclen)ZnOH	7.68	0.047 ± 0.001[a]	30
([15]aneN$_3$O$_2$)ZnOH	8.8	0.6 ± 0.06	28
([14]aneN$_4$)ZnOH	9.8		3a
(DPAS)ZnOH	8.6		21
(TPA)ZnOH	8.0		32
	Enzymes		
(E133A)Co^{II}PDF	6.5[b]		10
CAII	6.8 ± 0.1	2500 ± 200	34
(His94Cys)CAII	≥ 9.5	117 ± 20	34
LADH	9.2[c]		35

[a] 20 mM CHES (pH 9.3), $I = 0.1$ ($NaNO_3$), 10% (v/v) CH_3CN. [b] Determined by absorption spectroscopy. [c] This measurement is for the open, NADH-free enzyme.

Scheme 2

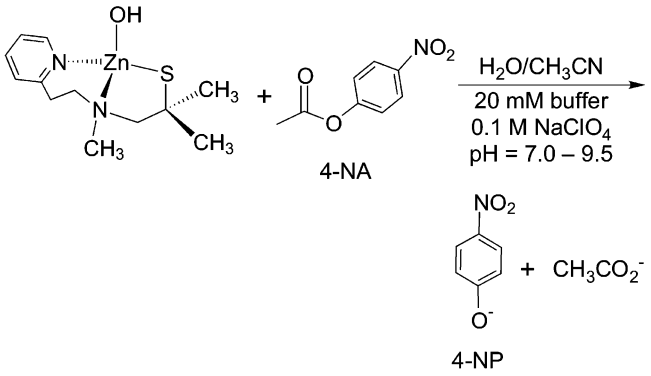

conditions (e.g., buffer, ionic strength) as close as possible to those used for kinetic measurements. The ^{1}H NMR spectrum of a solution of (PATH)Zn complex (10 mM) and 4-NA (10 mM) in D_2O (0.02 M HEPES-d_{18}, pH 8.2, 0.1 M $NaClO_4$) was recorded 5 min after mixing at room temperature, and showed the formation of free acetate (singlet at 2.07 ppm) and free nitrophenolate (two doublets at 6.80 and 8.24 ppm). Approximately 6% of the products 4-NP and acetate ion had formed at this point in the reaction. The peaks due to the zinc complex remained unchanged, and no other major peaks were observed. After 3 h more of the products had formed, and no other changes in the spectrum were observed. The only peaks observed 9 h after mixing corresponded to the cleavage products (acetate and nitrophenolate) and the zinc complex, indicating that all of the substrate 4-NA had been consumed. The ^{1}H NMR spectrum of **1** was recorded under the same conditions in the absence of substrate, and showed a spectrum identical to that of the zinc complex at the end of the hydrolysis reaction. Taken together these NMR data show that **1** cleanly reacts with the model substrate 4-NA to give the hydrolyzed products 4-NP and acetate ion according to Scheme 2.

Hydrolysis of 4-NA. Kinetics. The rate of hydrolysis of 4-NA was monitored by following the appearance of the

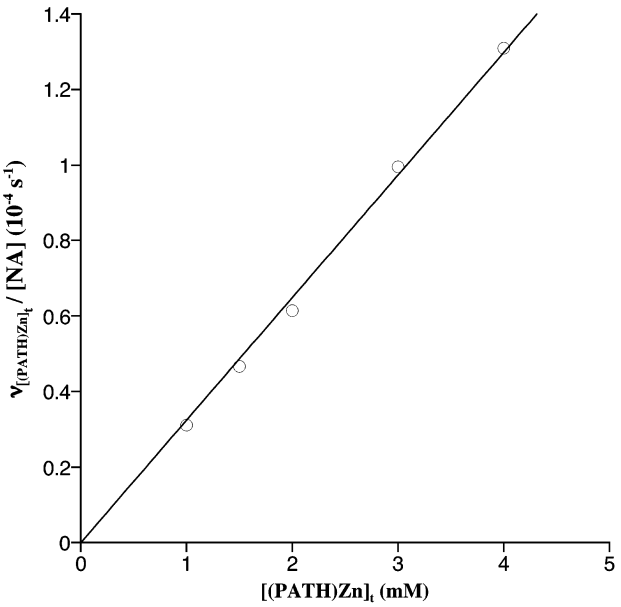

Figure 4. Dependence of $\nu_{[(PATH)Zn]_t}$/[NA] for the hydrolysis of 4-NA on [(PATH)Zn]$_t$ at pH 7.7 (20 mM HEPES), 25 °C, and $I = 0.10$ ($NaClO_4$).

nitrophenolate product by UV−vis spectroscopy. The rate constant for the hydrolysis of 4-NA by **1** (Scheme 2) was determined by the method of initial rates. This method works well for relatively slow reactions because only a small fraction of product (typically 1−3%) needs to be formed to obtain a good measure of the rate constant. The initial rate of hydrolysis (ν_{init}) of 4-NA by **1** was monitored up to ~3% conversion by following the increase in absorbance at 400 nm (λ_{max} for released 4-NP) over time. In all cases a plot of A_{400} versus time was clearly linear (0.990−0.999 correlation coefficient), and the slope yielded ν_{init}, the initial observed rate. The background rate of hydrolysis of 4-NA, ν_{buffer}, was measured independently under identical conditions in the absence of metal complex, and its effect on the total rate was eliminated by subtracting it from ν_{init} to give the rate of hydrolysis due to metal complex: $\nu_{[(PATH)Zn]_t} = \nu_{init} - \nu_{buffer}$.[22] The order of the reaction in both zinc complex and substrate was determined by measuring ν_{init} at different zinc complex concentrations with constant [4-NA] and different 4-NA concentrations with constant [(PATH)Zn]$_t$, respectively. A typical plot of $\nu_{[(PATH)Zn]_t}$/[4-NA] vs [(PATH)Zn]$_t$ at constant [4-NA] is shown in Figure 4, and is clearly linear, giving a slope equal to k_{obs}, the observed rate constant. Thus, it was concluded that the cleavage of 4-NA is first-order in both 4-NA and zinc complex, and leads to the straightforward second-order rate law given in eq 1,

$$\nu_{[(PATH)Zn]_t} = \nu_{init} - \nu_{buffer} = k_{obs}[(PATH)Zn]_t[NA] \quad (1)$$

where [(PATH)Zn]$_t$ = [(PATH)Zn(OH$_2$)]$^+$ + [(PATH)-ZnOH] in the pH range studied.

pH−Rate Profile for the Hydrolysis of 4-NA. The observed second-order rate constants, k_{obs} (M^{-1} s^{-1}), were obtained by the method described above over a range of pH

(22) Li, S. A.; Xia, J.; Yang, D. X.; Xu, Y.; Li, D. F.; Wu, M. F.; Tang, E. X. *Inorg. Chem.* **2002**, *41*, 1807−1815.

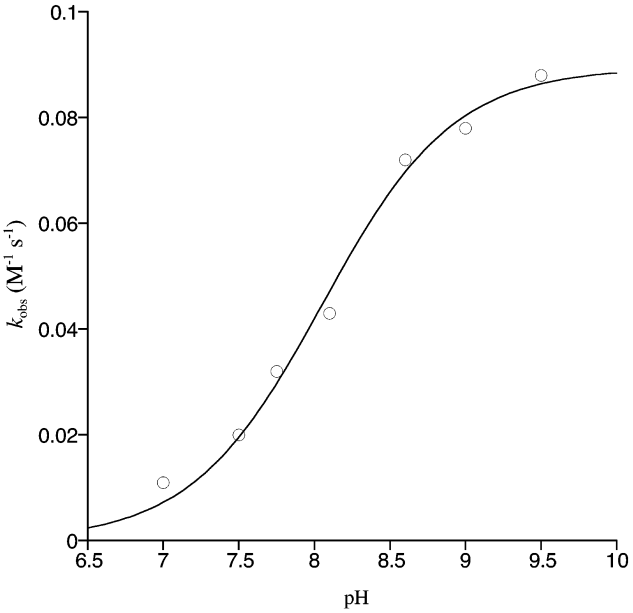

Figure 5. pH−rate profile for the hydrolysis of 4-NA by (PATH)ZnOH at 25 °C and $I = 0.10$ ($NaClO_4$) in 10% CH_3CN aqueous solution.

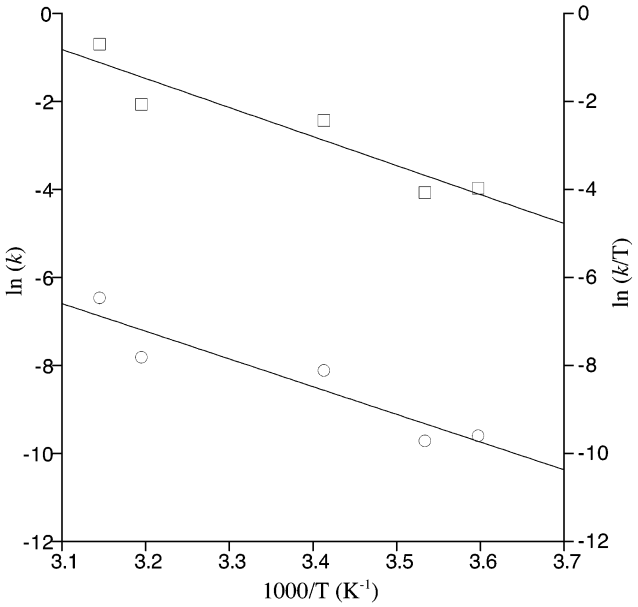

Figure 6. Effect of temperature on the hydrolysis of 4-NA by (PATH)-ZnOH in the form ln k vs $1/T$ (bottom, left y axis) (squares) and ln(k/T) vs $1/T$ (bottom, right y axis) (circles). Initial concentrations of the complex and substrate were 3.5×10^{-4} and 1.0×10^{-3} M, respectively. The solvent was a 9:1 mixture of H_2O and CH_3CN with 0.02 M CHES buffer (pH 8.75) and $I = 0.10$ ($NaClO_4$).

values. In Figure 5 is shown a plot of k_{obs} versus pH. The rate constant clearly increases with increasing pH up to ∼9.5. This curve immediately suggests that the formation of the catalytically active species involves the removal of a proton, and is similar to the pH−rate profiles of other zinc model complexes for which the active catalytic species is a nucleophilic ZnOH complex. In general terms, the curve in Figure 5 is indicative of a reaction system in which there is a rapidly established acid−base equilibrium prior to a slow step which controls the kinetics, and this system can be represented by eqs 2−4.[23]

$$[(PATH)ZnOH_2]^+ \overset{K_a}{\rightleftharpoons} (PATH)ZnOH + H^+ \qquad (2)$$

$$(PATH)ZnOH + 4\text{-}NA \xrightarrow{k''_{max}} \text{products} \qquad (3)$$

$$k_{obs} = k''_{max}K_a/(K_a + [H^+]) \qquad (4)$$

The expression for k_{obs} in eq 4 was employed in fitting the curve in Figure 5, and the K_a and k''_{max} parameters were refined in a nonlinear least-squares fitting procedure to give $pK_a = 8.05(5)$ and $k''_{max} = 0.089(3)$ M^{-1} s^{-1}. The kinetic pK_a of 8.05(5) is in agreement with the thermodynamic pK_a obtained from the potentiometric titration measurements. The k''_{max} value of 0.089(3) M^{-1} s^{-1}, which corresponds to the pH-independent rate constant, provides a direct measure of the hydrolytic efficiency, and hence nucleophilicity, of the active catalytic species, **1**.

Temperature Dependence of the Hydrolysis of 4-NA. The effect of temperature on the observed rate constant, k_{obs}, was measured over the temperature range 5−45 °C at pH 8.75, where the zinc complex is in mostly the hydroxide form. A plot of ln(k_{obs}) versus $1/T$ is shown in Figure 6, and is clearly linear, exhibiting behavior consistent with the Arrhenius equation.[24] The slope obtained from the best-fit line of these data yields the activation energy (slope $= -E_a/R$). A plot of ln(k_{obs}/T) versus $1/T$ is also linear and corresponds to an Eyring plot, from which the best-fit line gives the activation parameters $\Delta H^‡$ (slope $= -\Delta H^‡/R$) and $\Delta S^‡$ (y intercept $= [\ln(k_b/h)] + \Delta S^‡/R$).[24] The values found for the activation parameters are given in Table 3 along with values obtained for the zinc complexes of [12]aneN_3[25] and cyclen,[26] as well as the tris(pyrazolyl)borate complex ($Tp^{Cum,Me}$)ZnOH[27] (Chart 1).

Table 3. Activation Parameters for 4-NA Hydrolysis

	E_a (kJ mol^{-1})	$\Delta H^‡$ (kJ mol^{-1})	$\Delta S^‡$ (J mol^{-1} K^{-1})	ref
(PATH)ZnOH	54.8	52.4	−90.0	this work
($Tp^{Cum,Me}$)ZnOH	64.3	61.8	−85.6	27
([12]aneN_3)ZnOH	49 ± 2			25
(cyclen)ZnOH	45 ± 2			26
OH^-	43 ± 2			26

Turnover. To determine whether **1** could function as a catalyst in the hydrolysis of 4-NA, we performed the following turnover experiment. The hydrolysis reaction was run with a 50-fold excess of substrate at pH 8.6 and monitored by UV−vis spectroscopy. A control reaction was monitored at the same time with conditions that were identical except that no metal complex was present. Aliquots of the reaction mixture were removed at regular intervals for monitoring the production of 4-NP at 400 nm. A greater

(23) Zuman, P.; Patel, R. C. *Techniques in Organic Reaction Kinetics*; John Wiley & Sons: New York, 1984.

(24) Wilkins, R. G. *Kinetics and Mechanism of Reactions of Transition Metal Complexes*; VCH Publishers: New York, 1991.

(25) Kimura, E.; Nakamura, I.; Koike, T.; Shionoya, M.; Kodama, Y.; Ikeda, T.; Shiro, M. *J. Am. Chem. Soc.* **1994**, *116*, 4764−4771.

(26) Koike, T.; Takamura, M.; Kimura, E. *J. Am. Chem. Soc.* **1994**, *116*, 8443−8449.

(27) Rombach, M.; Maurer, C.; Weis, K.; Keller, E.; Vahrenkamp, H. *Chem.—Eur. J.* **1999**, *5*, 1013−1027.

than stoichiometric amount of 4-NA was hydrolyzed by **1**; after 1 week about seven turnovers were observed after the hydrolysis from the background reaction was accounted for. Moreover, from kinetic measurements we determined that at pH 8.6 the metal-promoted reaction is 16 times faster than the background reaction due to free OH^-. Although the turnovers are modest, these data, combined with the observed rate enhancement over the background reaction, indicate that **1** behaves as a catalyst for the hydrolysis of 4-NA under these conditions.

Discussion

Synthesis. The hydroxide complex **1** can be generated in aqueous solution by protonolysis of the zinc methyl complex **2** or via titration of an aqueous solution of PATH−H·2HNO_3 and $Zn(NO_3)_2$ with NaOH. The ^{1}H NMR data confirm that the same species is formed in either case. We preferred to use the method involving the zinc methyl complex for all of the reactivity studies because it results in clean solutions of **1** derived from the structurally well-defined precursor **2**, and because of the convenient nature of simply weighing out **2** as a stable solid and dissolving it in water to give a known concentration of the active hydroxide species.

Formation Constant and pK_a of the Coordinated Water Molecule. The formation constant for $[(PATH)Zn]^+$ (log K(ZnL) = 10.35(5)) and the pK_a of the bound water molecule (pK_a = 7.7(1)) obtained from the potentiometric titration are given in Table 1. For comparison, the formation constants for some of the other ligands shown in Chart 1 are also collected in Table 1. The large formation constant for PATH (log K(ZnL) = 10.35(5)) is considerably higher than that of the macrocyclic tridentate N donors [12]aneN_3[3a] and [15]aneN_3O_2,[28,29] and shows that the $[(PATH)Zn]^+$ complex is extremely stable in aqueous solution. The high K(ZnL) for PATH is likely a consequence of the presence of the basic thiolate donor. However, the N_4 macrocyclic ligands cyclen[30] and [14]aneN_4[3a] exhibit significantly higher formation constants than PATH, both of which benefit from a fourth donor atom and the added stability of a macrocyclic framework.

The most significant finding is the protonation constant for **1**, pK_a = 7.7(1). To our knowledge this is the first time the pK_a value of a water molecule bound to a N_2S(thiolate)-Zn^{II} center outside of a protein has been measured. As is typical of the zinc model compounds in Chart 1, the pK_a for **1** is considerably lower than that of $Zn(H_2O)_6^{2+}$ (pK_a = 9.0).[31] In comparison, it is slightly higher than the pK_a = 7.3 for ([12]aneN_3)ZnOH. Given that PATH and [12]aneN_3 present the same number of donor atoms, we can readily attribute the increase in pK_a for the PATH complex to the presence of the negatively charged thiolate donor, which puts more electron density on the metal center and causes a resultant decrease in Lewis acidity. Interestingly, the pK_a for **1** is very similar to that of the zinc complexes of cyclen (pK_a = 7.9) and TPA[32] (pK_a = 8.0), suggesting that the incorporation of RS^- into a tridentate donor ligand has an effect on the pK_a similar to that of adding a fourth nitrogen donor to the zinc coordination sphere. In keeping with this trend, (DPAS)ZnOH, which contains a negatively charged thiolate group in addition to a fourth N donor, exhibits a slightly higher pK_a (8.6) than **1** or its all-nitrogen analogue (TPA)ZnOH. In general, the influence of coordination number and donor type (e.g., neutral versus charged) over the pK_a of zinc model complexes and zinc enzymes has been of great interest, but there have been no systematic studies outside of theoretical calculations,[33] in part because of a lack of suitable model complexes with different types and numbers of donor atoms. Our findings for a N_2S(thiolate)-ZnOH complex help to fill in this gap and are in line with the trends observed in the latter theoretical study, which indicate that the pK_a increases with an increase in coordination number or addition of negatively charged ligands. However, there are other effects besides donor atom type and number that appear to have a profound influence on Lewis acidity. For example, the very high pK_a (9.8) of the [14]aneN_4 complex in Chart 1 has been ascribed to subtle geometric effects at the metal.[3a] In addition, the zinc complex of the N_3 donor [15]aneN_3O_2 exhibits a relatively high pK_a (8.8), and it has been suggested that weak O atom coordination as well as H-bond formation between the polyoxa chain and the coordinated water molecule accounts for the high pK_a of this complex.[29] It is clear from our model system that the presence of a thiolate donor in the coordination sphere of Zn^{II} will cause a modest increase in the pK_a of the coordinated water molecule. However, donor type and number do not always dominate the pK_a value; there are other subtle structural features that can cause the pK_a to shift significantly, and as discussed below, the unusually low pK_a for a mutant form of PDF reinforces this idea.

The pK_a values for the zinc enzymes CAII[34] and LADH[35] and a mutant form of cobalt(II)-substituted PDF[10] are given in Table 2. CAII and LADH contain zinc centers with His_3 [N_3] and $HisCys_2$ [NS_2(thiolate)] donor sets, respectively, and are well-studied representatives of the mononuclear zinc enzyme family. The native CAII enzyme has a pK_a of 6.8.[34] Upon mutation of a zinc-ligated histidine to cysteine ((His94Cys)CAII),[34] the pK_a of the coordinated water molecule increases dramatically to p$K_a \geq$ 9.5.[34] Likewise, the ZnOH moiety of LADH exhibits a pK_a of 9.2.[35] Although the pK_a of wild-type Co^{II}PDF is complicated by the H-bonding interaction with Glu-133 (Figure 1), a pK_a of 6.5 has been measured for (E133A)CoPDF, which has no

(28) Bazzicalupi, C.; Bencini, A.; Bianchi, A.; Fusi, V.; Giorgi, C.; Paoletti, P.; Valtancoli, B.; Zanchi, D. *Inorg. Chem.* **1997**, *36*, 2784−2790.
(29) Bazzicalupi, C.; Bencini, A.; Bencini, A.; Bianchi, A.; Corana, F.; Fusi, V.; Giorgi, C.; Paoli, P.; Paoletti, P.; Valtancoli, B.; Zanchini, C. *Inorg. Chem.* **1996**, *35*, 5540−5548.
(30) Koike, T.; Kajitani, S.; Nakamura, I.; Kimura, E.; Shiro, M. *J. Am. Chem. Soc.* **1995**, *117*, 1210−1219.
(31) Sigel, H.; Martin, R. B. *Chem. Soc. Rev.* **1994**, 83−91.
(32) Anderegg, G.; Hubmann, E.; Podder, N. G.; Wenk, F. *Helv. Chim. Acta* **1977**, *60*, 123−140.
(33) Bertini, I.; Luchinat, C.; Rosi, M.; Sgamellotti, A.; Tarantelli, F. *Inorg. Chem.* **1990**, *29*, 1460−1463.
(34) Kiefer, L. L.; Fierke, C. A. *Biochemistry* **1994**, *33*, 15233−15240.
(35) Bertini, I.; Luchinat, C. In *Bioinorganic Chemistry*; Bertini, I., Gray, H. B., Lippard, S., Valentine, J., Eds.; University Science Books: Mill Valley, CA, 1994; pp 37−106.

Scheme 3

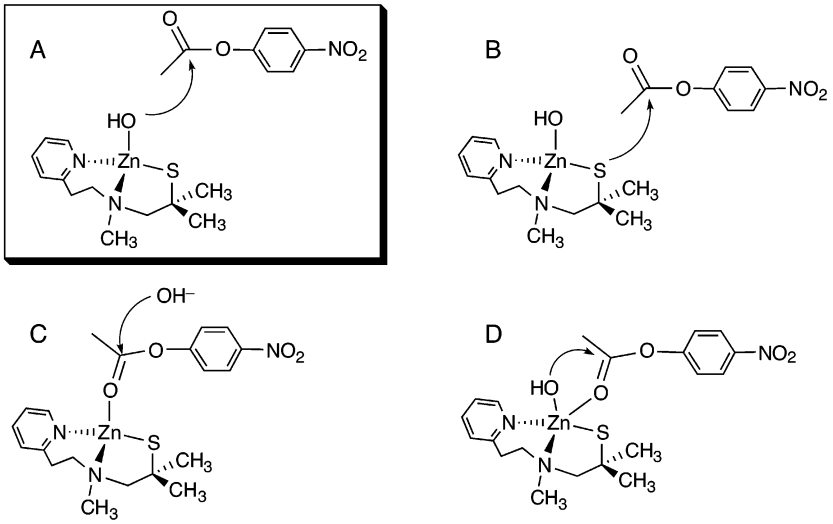

H-bond and therefore provides the intrinsic pK_a of the metal-bound water molecule.[10] This pK_a is *2−3 units below* that of **1** as well as (His94Cys)CAII, and is clearly not in line with the trends exhibited by the complexes and enzymes given in Table 2. One would expect the pK_a for Co^{II}-substituted PDF to be *slightly higher than* that for **1** simply on the basis of the inherent effect of the different metal ions; compare the acidity of free Zn^{II}, p$K_a(Zn(H_2O)_6^{2+}) = 9.0$,[31] versus free Co^{II}, p$K_a(Co(H_2O)_6^{2+}) = 9.8$.[36] Thus, there must be certain as yet unidentified features outside of the first coordination sphere of (E133A)CoPDF that dramatically increase the acidity of the $M^{II}OH_2$ unit.

Hydrolysis of 4-NA. ^{1}H NMR Analysis, Kinetics, and Mechanism. Monitoring the reaction between (PATH)ZnOH and 4-NA by ^{1}H NMR spectroscopy shows that 4-NA is cleanly hydrolyzed to 4-NP and acetate ion. After 5 min of mixing, the reaction mixture shows only hydrolyzed products and unreacted substrate and metal complex. As the reaction proceeds, the only changes in the NMR spectrum correspond to an increase in 4-NP and acetate and a decrease in the substrate. The pathways shown in Scheme 3 characterize possible mechanisms for the hydrolysis. The NMR data are consistent with the simple nucleophilic attack mechanism shown in Scheme 3A. Recent work on zinc hydroxide model complexes containing coordinated alkoxide groups has implicated the alkoxide moiety as the initial reactive nucleophile in the cleavage of 4-NA.[25,30,37] The main evidence for this mechanism comes from NMR data, which show the presence of a transient acetyl intermediate in which the alkoxide donor has formed an ester with the carboxylate group of the substrate.[25,30,37] Although the alkylthiolate group of PATH could potentially act as a nucleophile, we see no evidence of a thioester intermediate by NMR, arguing against the mechanism in Scheme 3B. It is likely that the nucleophilicity of the alkylthiolate is significantly reduced by the *gem*-dimethyl substituents near the sulfur atom. These groups were originally incorporated into PATH to sterically block the formation of M−S(R)−M bridged structures, and they most likely impose sufficient steric crowding near the free S lone pair so as to deter sulfur-based nucleophilic attack.

The ability of **1** to promote significant rate enhancement for the hydrolysis of 4-NA in the pH range 7.0−9.5 has been established by the kinetic measurements. For example, at pH 8.6, **1** is 16 times more effective ($\nu_{[(PATH)Zn]_t}/\nu_{buffer}$; $[(PATH)Zn]_t = 4$ mM) at hydrolyzing 4-NA than buffered solution in the absence of zinc complex. The sigmoidal shape of the pH−rate profile in Figure 5 is consistent with the mechanism shown in Scheme 3A, where the active catalytic species is the zinc hydroxide complex, and simple nucleophilic attack of the metal-bound hydroxide facilitates hydrolysis of the substrate. Alternative mechanisms for metal-promoted hydrolysis include electrophilic activation of 4-NA through precoordination (Scheme 3C), or both electrophilic activation and nucleophilic attack in a hybrid-type mechanism (Scheme 3D).[1,38,39] The rate enhancement factor ($\nu_{[(PATH)Zn]_t}/\nu_{buffer}$) and second-order rate constant (k''_{max}) for (PATH)ZnOH are quite similar to those of the other zinc complexes in Table 2 for which rate constants are given, and which have previously been described to operate through simple nucleophilic attack (Scheme 3A) of 4-NA. Pathways C and D of Scheme 3 depend on strong binding and electrophilic activation of the substrate, and we see no evidence of binding by NMR. In addition, we would expect the hybrid mechanism (Scheme 3D) to lead to a much larger value of k''_{max}, larger than even that of free OH^-.[40,41] We also conducted a control experiment between **3** and 4-NA to test whether an electrophilic activation mechanism could be induced given a complex lacking a metal-bound hydroxide ligand. The very low solubility of **3** (Scheme 1) in water precluded us from carrying out this reaction in an aqueous

(36) Sillén, L. G.; Martell, A. E. *Stability Constants of Metal-ion Complexes*; Special Publication of the Chemical Society: London, 1971; Vol. 25.
(37) Bazzicalupi, C.; Bencini, A.; Berni, E.; Bianchi, A.; Fedi, V.; Fusi, V.; Giorgi, C.; Paoletti, P.; Valtancoli, B. *Inorg. Chem.* **1999**, *38*, 4115−4122.
(38) Hegg, E. L.; Burstyn, J. N. *Coord. Chem. Rev.* **1998**, *173*, 133−165.
(39) Sayre, L. M. *J. Am. Chem. Soc.* **1986**, *108*, 1632−1635.
(40) Gellman, S. H.; Petter, R.; Breslow, R. *J. Am. Chem. Soc.* **1986**, *108*, 2388−2394.
(41) Koike, T.; Kimura, E. *J. Am. Chem. Soc.* **1991**, *113*, 8935−8941.

solution, but it was sufficiently soluble in an acetonitrile/water mixture. A solution of **3** (0.11 mM) and 4-NA (0.22 mM) in CD_3CN/D_2O (90:10 v/v) was monitored by ^1H NMR spectroscopy, and showed no reaction after 24 h. These data suggest that the (PATH)Zn^{II} unit does not readily bind 4-NA and activate it toward hydrolysis via an electrophilic mechanism, adding further support for the mechanism in Scheme 3A.

It is of interest to compare the hydrolytic efficiency of **1** with those of the other model complexes for which a rate constant is given in Table 2. All of these complexes exhibit the same sigmoidal pH−rate profile and increase in rate with pH as seen for **1**. The rate constants in Table 2 were selected from the literature to correspond as closely as possible to k''_{max} (the pH-independent rate constant) for these complexes. The k''_{max} value of 0.089(3) M^{-1} s^{-1} for **1** is approximately double that of ([12]aneN_3)ZnOH (0.036 ± 0.003 M^{-1} s^{-1}) and (CH_3cyclen)ZnOH (0.047 ± 0.001 M^{-1} s^{-1}), but similar to that of (cyclen)ZnOH (0.1 ± 0.01 M^{-1} s^{-1}), and considerably lower than that for [15]aneN_3O_2 (0.6 ± 0.06 M^{-1} s^{-1}). The hydrolytic efficiency clearly correlates with an increase in the basicity of the ZnOH unit for these complexes, and is in keeping with the rate-determining step involving nucleophilic attack (Scheme 3A). It is safe to conclude from these data that the alkylthiolate donor (RS^-) of PATH increases the hydrolytic efficiency, and therefore the nucleophilicity of the ZnOH unit as compared to the tridentate [N_3] donor ligand in ([12]aneN_3)ZnOH. The presence of RS^- has an effect similar to that caused by the addition of a fourth N donor, as found in the cyclen complex. The relatively low reactivity of the CH_3cyclen complex may be a consequence of the steric hindrance imposed by the CH_3 group, which presumably lowers the nucleophilicity of the ZnOH unit.[30] Interestingly, the pH-independent rate constant for free OH^- (9.5 M^{-1} s^{-1}) is approximately 2 orders of magnitude larger than that of any of these zinc model complexes. This observation is in keeping with Scheme 3A representing the rate-determining step and the expectation that the best "simple" nucleophile is free OH^-. Thus, the zinc center in both models and proteins functions to activate water and generate a powerful nucleophile at relatively low concentration of free OH^-.

The dependence of the rate constant on temperature was examined to obtain activation parameters and gain more information concerning the mechanism of hydrolysis of 4-NA. The activation parameters listed in Table 3 were obtained from the Arrhenius and Eyring plots in Figure 6. To our knowledge, the only activation energies (E_a) that have been measured for zinc-promoted hydrolysis of 4-NA are those given in Table 3, and $\Delta H^{\ddagger}$ and $\Delta S^{\ddagger}$ for L_nZnOH-promoted ester hydrolysis have only been measured previously for the tris(pyrazolyl)borate complex ($Tp^{Cum,Me}$)-ZnOH.[27] All of the activation energies given in Table 3 are relatively close to each other, suggesting a similar mechanistic scheme for all of the complexes. In the previous study of ($Tp^{Cum,Me}$)ZnOH, it was proposed that the mechanism of hydrolysis of 4-NA by this complex and other L_nZnOH species involves a four-centered transition state that arises from the hybrid mechanism shown in Scheme 3D, and not the simple nucleophilic attack mechanism of Scheme 3A. This proposal was based on the similarity of the activation parameters for 4-NA hydrolysis with those obtained in the same study for the hydrolytic cleavage of organophosphate esters. It was argued that the activation entropies (−54 to −126 J mol^{-1} K^{-1}) obtained for the organophosphate substrates had to be considered large compared to that of a "typical" bimolecular process, and were the best experimental evidence supporting the notion that the transition state had an unusually high degree of ordering. It is not clear to us why these activation entropies were considered particularly large, since there are no comparative $\Delta S^{\ddagger}$ values available for similar L_nZnOH-promoted hydrolysis of either organophosphates or esters. However, as has been shown by others, a hybrid mechanism is likely operative in the case of organophosphates in part because of the large rate constants obtained for L_nZnOH hydrolysis as compared to the rate constant for free hydroxide (e.g., $k_{(OH)} = 2.8 \times 10^{-2}$ M^{-1} s^{-1} vs $k_{((L)ZnOH)} = 2.8 \times 10^{-1}$ M^{-1} s^{-1}).[28,40,41] It is highly unlikely that any L_nZnOH species is a better inherent nucleophile than free OH^-, and therefore, a simple nucleophilic attack mechanism would not explain the much larger L_nZnOH rate constants. Thus, a hybrid mechanism is reasonably invoked for organophosphate hydrolysis. However, the rate constants for zinc complex-promoted hydrolysis of various ester substrates are invariably *smaller* than those for simple alkaline hydrolysis, as is found for the PATH complex and the other entries of Table 2. It must be noted that the hydrolytic study involving ($Tp^{Cum,Me}$)ZnOH was carried out in nonaqueous solvent (chloroform) for both organophosphates and 4-NA, and therefore, direct comparison of rate constants with that of free OH^- cannot be made. In any case, we do not find the $\Delta S^{\ddagger}$ value for the hydrolysis of 4-NA by **1** to be out of the ordinary; indeed, the simple alkaline hydrolysis of CH_3CO_2Ph has $\Delta S^{\ddagger} = -92$ J mol^{-1} K^{-1}.[42,43] The large negative value of the activation entropy is indicative of an associative mechanism in which the rate-determining step is similar to Scheme 3A, but does not necessarily imply any further ordering of the transition state as might be expected if Scheme 3D were operative. If a four-centered transition state were involved, one would expect a significantly more negative $\Delta S^{\ddagger}$ for **1** than for free OH^-. Moreover, a phosphorus center can accommodate the geometric requirements of a four-center transition state without much difficulty, whereas the carbon center of an ester should exhibit significantly more strain.[40] Thus, the temperature-dependent studies, the pH−rate profile, the NMR studies, and all rate constants and activation parameters support the mechanism of Scheme 3A.

Although **1** exhibits slow turnover, we were able to observe greater than stoichiometric hydrolysis of 4-NA, implying that **1** does indeed function as a catalyst. We attempted to inhibit turnover by the addition of an excess of 4-NP, and observed a small effect on turnover number

(42) Isaacs, N. *Physical Organic Chemistry*, 2nd ed.; John Wiley & Sons: New York, 1995.
(43) Jencks, W. P.; Gilchrist, M. *J. Am. Chem. Soc.* **1968**, *90*, 2622−2637.

(~30% decrease) with the addition of 10 equiv of 4-NP to the reaction mixture. These data suggest that *p*-nitrophenolate, when present in excess, exhibits weak binding toward **1**.

Concluding Remarks

The results described here provide for the first time a measure of the basicity and hydrolytic efficiency of a zinc ion in a N_2S(thiolate) environment. In this regard, **1** exhibits a pK_a and pH-independent second-order rate constant for hydrolysis of 4-NA that are both in line with those of other monomeric zinc model complexes. The thiolate donor of PATH increases the pK_a and nucleophilicity of the MOH unit to a modest extent as expected from comparison with the other model complexes. The significantly low pK_a of the metal-bound water molecule in the active site of (E133A)-CoPDF remains unexplained. The data for **1**, together with the data for the other zinc models and enzymes in Table 2, suggest that there must be some subtle but as yet unidentified active site features of PDF that cause the pK_a to be so much lower than expected. The NMR studies and the kinetic profile point to a mechanism for the hydrolysis of 4-NA in which **1** acts as a simple nucleophile in the rate-determining step. Such a result is not unexpected given that a similar mechanism has been proposed for several of the other zinc model complexes of Chart 1. In addition, the activation parameters obtained for this reaction are consistent with the simple associative mechanism proposed. The E_a, $\Delta H^{\ddagger}$, and $\Delta S^{\ddagger}$ for hydrolysis of an ester by a zinc complex have been measured in only one other case,[27] and in this study it was concluded that the mechanism of hydrolysis was a hybrid-type mechanism as shown in Scheme 3D, in contrast to the analysis presented here. Our results suggest that the ZnOH unit, once generated in the PDF active site, should be a perfectly competent and well-behaved nucleophile for attack of the formamide substrate, and imply that the cause of the remarkably low reactivity of ZnPDF lies elsewhere.

Acknowledgment. We are grateful to the National Institutes of Health (Grant GM62309 to D.P.G.) for support of this work. D.P.G. acknowledges the Alfred P. Sloan, Jr. Foundation for an Alfred P. Sloan, Jr. Research Fellowship.

IC034337O